Effects of flight parameters for plant protection UAV on droplets deposition rate based on a 3D simulation approach

Lifeng Xu[1*], Zhongzhu Yang[1], Zusheng Huang[1], Weilong Ding[1], Gerhard Buck-Sorlin[2]

(1. *College of Computer Science & Technology, Zhejiang University of Technology, Hangzhou 310026, China*;
2. *IRHS, INRAE, AGROCAMPUS OUEST, Universit́e d'Angers, SFR 4207 QUASAV, 42 rue Georges Morel, 49071 Beaucouzé cedex, France*)

Abstract: With the development of aviation agricultural technology, the number of farmers adopting the use of drones in daily agricultural activities is growing rapidly in recent decades. Among these, a large portion constitutes agricultural drones being used in pest control and crop protection practices, e.g. agriculture spraying of pesticides. Spraying pesticides with drones have proven to be faster than other traditional methods. On the downside, flight time and range of Unmanned Aerial Vehicles (UAV) are often limited. Thus, a proper arrangement of flight height and velocity will greatly improve spraying efficiency. A new strategy to optimize the flight parameters, i.e. flight height and flight velocity, for fixed-wing UAV with a 3D simulation-based approach together with an automatic optimization algorithm was proposed in this study. To find the optimal parameters for a UAV to fly and spray under certain environmental conditions, a three-dimensional model of the target crop was established first, followed by a detailed simulation of droplet spraying. As a demonstration case, a grass model was developed and used as the target plant, and a physics-based method was used to simulate realistically the movement of the droplets in the air as well as the interaction between the droplets and the plant to obtain the droplet deposition rate under the specified operating parameters. Furthermore, the standard Particle Swarm Optimization (PSO) algorithm was used to optimize the UAV operating parameters to obtain the best operating parameters. The results indicate that using the standard PSO algorithm to optimize the operating parameters of the drone could significantly improve the deposition rate and find the best operating parameters.

Keywords: unmanned aerial vehicle, droplet deposition, 3D simulation, particle swarm optimization algorithm
DOI: 10.25165/j.ijabe.20231601.6581

Citation: Xu L F, Yang Z Z, Huang Z S, Ding W L, Buck-Sorlin G. Effects of flight parameters for plant protection UAV on droplets deposition rate based on a 3D simulation approach. Int J Agric & Biol Eng, 2023; 16(1): 66–72.

1 Introduction

The development of agriculture is of great significance to the progress of society[1]. Pests and diseases still have a great negative impact on crop growth and directly reduce yield and quality[2]. Therefore, agricultural development and crop protection have always been inseparable. A major method of crop protection is spraying pesticides on crops, with several advantages, including high speed, wide range, and low cost. Pests and diseases can be effectively controlled and the negative effect of pests and diseases on crop yields be reduced.

In the process of spraying pesticides, only a small part of the liquid solution settles on the crop surface, while most of the liquid gets into the surrounding environment causing environmental pollution[3]. With the development of air spraying technology, more and more agricultural Unmanned Aerial Vehicles (UAVs) have begun to be applied in pest control work[4]. Aerospray has the following advantages: 1) The agricultural drone has a larger spray volume and can spray a large area quickly; 2) A drone flying above the crop will not cause damage to the crop the way a wheeled vehicle on the ground does; 3) UAVs can work normally in mountainous areas, hills, and other inaccessible environments, and the working efficiency is a dozen times that of ground-mounted motorized sprayers[5].

However, aerospray still has a series of problems such as uncertain operating parameters (velocity and height of UAV), low spraying efficiency, and the need for optimization of UAV routes. The setting of drone operation parameters can directly affect droplet deposition distribution[6]. Franz et al.[7] sprayed fluorescent tracers instead of pesticides on fixed-wing aircraft. The effects of crop canopy characteristics and environmental factors on the deposition of droplets on leafy plants such as cotton and Hami melon were studied. Under the spraying operation of a fixed-wing aircraft, Lan et al.[8] studied the effects of different working heights and additive concentrations on droplet deposition and drift. Kirk et al.[9] studied the relationship between flight speed, nozzle flow rate, spray pressure, droplet size, and other factors, and established a mathematical model capable of predicting droplet deposition and drift. Fritz et al.[10,11] evaluated the effects of wind fields and nozzles on aerospace spray deposition and drift distribution. Huang et al.[12] tested how different factors such as wind speed, release height, and droplet size affected droplet deposition distribution and selected the maximum influence factor to control and reduce the drift of the droplets. Faical et al.[13,14]

Received date: 2021-08-16 **Accepted date:** 2022-03-17
Biographies: Zhongzhu Yang, Master candidate, research interest: plant modeling and virtual simulation, Email: zhongzhu_yang@126.com; **Zusheng Huang**, Master candidate, research interest: plant modeling and optimization algorithm, Email: zusheng.h@outlook.com; **Weilong Ding**, PhD, research interest: virtual plant modeling, Email: wlding@zjut.edu.cn; **Gerhard Buck-Sorlin**, PhD, research interest: plant modeling, Email: gerhard.buck-sorlin@agrocampus-ouest.fr.
***Corresponding author: Lifeng Xu**, PhD, research interest: virtual plant modeling. College of Computer Science & Technology, Zhejiang University of Technology, Hangzhou 310026, China. Tel: +86-571-85290527, Email: lfxu@zjut.edu.cn.

considered the effect of weather conditions on the distribution of droplet deposition. The weather conditions were obtained by using a Wireless Sensor Network (WSN). A parameter called 'routeChangingFactor' was proposed to correct the flight route of UAV. Particle Swarm Optimization and Genetic Algorithm were used in those studies to obtain the optimal parameterization during the spraying operation of the UAV, While a multiple regression model was used to predict the optimal spraying height and flight speed in citrus trees using a quadrotor UAV[15].

Particle Swarm Optimization (PSO)[16] is a bionic intelligence optimization algorithm. PSO simulates the foraging process of birds in nature. Individuals in the flock are looking for food in different directions. When the food location is found, the information of food location will be shared in the flock. Then the flock will move toward the food location. In the particle swarm optimization algorithm, each particle in the population represents a feasible solution to the optimization problem, and the food position represents the optimal solution of the optimization problem. In order to find the food location, the entire population continuously explores the solution space. In the process of exploration, all individuals move continuously through their own search experience and the search experience of other individuals in the population. In the algorithm optimization process, a single particle adjusts the position and velocity of the particle through its own historical optimal value and the historical optimal value of the population determines the fitness function according to the actual optimization problem and determines the optimal value through the fitness function.

All the above studies were conducted in a real-world drone-spraying test, which allowed this study to obtain the best operating parameters for a particular type of crop under specified external environmental conditions. However, conditions encountered when practicing spraying in the field might considerably deviate from the experimental environmental conditions. Therefore, the results of the test for the actual spraying operations are relatively weak. For this reason, the present study proposes a 3D simulation based optimization method for drone operation parameters used in a plant protection context, which can provide theoretical guidance for dredging operations under different types of crops and under different environmental conditions. First, a three-dimensional model of a given crop based on user needs was established and external environmental conditions were initialized. Then a physics-based method was used to provide a realistic simulation of the movement of the droplets in the air and the interaction between the droplets and the crop to obtain the droplet deposition rate under the specified operating parameters. Finally, the standard particle-swarm optimization algorithm[16] was used to optimize automatically the UAV operating parameters.

2 Method

2.1 3D plant and spray model

A *Gramineae* model, Fat hen to be specific, was established to demonstrate the implementation results for the optimization workflow. Plants of the grass family are during their vegetative state composed of a rosette of leaves inserted on a very short stem. Each leaf is composed of a sheath and a blade, the latter being the exposed part that will normally also receive the bulk of the sprayed pesticide. For our purposes, the leaf was simplified to the visual representation of a blade, as an ensemble of four quadrangles. The number of leaves per individual grass was set to a random value between 8 and 12. The range for the length of the leaves was 20-30 cm and the width was 1-2 cm. Grass blades in the real world are usually flat and curved. The geometry of the grass blade can be approximated using a quadrilateral strip. A single grass blade can be divided into multiple segments. Each segment is represented by a quadrilateral (as shown in Figure 1). The cubic Bezier curve could be used to describe the bending and smoothing properties of grass blade (Figure 2). The control vertices of cubic Bezier curve were used to control the degree of grass blade. The cubic Bezier curve[17] $B(n)$ was defined as follows:

$$B(n) = (1-n)^3 P_v^0 + 3(1-n)^2 n P_v^1 + 3(1-n) n^2 P_v^2 + n^3 P_v^3 \quad (1)$$

where, P_v^0, P_v^1, P_v^2, and P_v^3 represent the control vertices of cubic Bezier curve (v as vertex), and n indicates the interpolation parameter from the top of grass blade to the bottom.

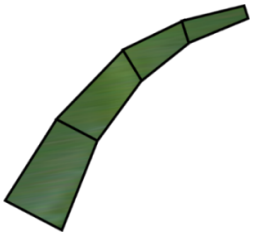

Figure 1 Segmentation of grass blade

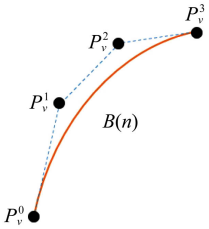

Figure 2 Representation of grass model

In the real spray scene, new droplets are continuously generated and the droplets disappear after falling into the ground. Particle system was used to simulate spray scene. A large number of simple-shaped particles were built into the particle system. Each particle was always in motion before the end of its life cycle. Particle systems can be used to simulate objects that are irregularly shaped and constantly changing, such as flames, water, and fireworks. In a particle system, the object to be simulated consists of a large number of particles, each with its own life cycle, and the particles move during the life cycle. The object is simulated by updating the properties of the particle during its movement. In this paper, a single droplet was used as a particle in the particle system. Droplet particles have properties such as position, velocity, acceleration, and diameter. Droplets stopped moving after falling into the ground and were then removed from the particles list. Specific steps are as follows:

1) Initialization. At the beginning of the algorithm, the position of the nozzle and the flow rate of the nozzle was initialized, and the initial velocity and diameter of the droplet particles were set according to the type of the nozzle.

2) Updating. The position and velocity of the droplets were updated in each time step. Droplets and blades collided in real-time. If no collision occurred, the droplet continued to move in the air; in the event of a collision, the state of the droplet after the collision was determined according to the determination conditions in the droplet collision process.

3) Disappearing. There were two conditions for determining the demise of particles in this study. Droplet particles were

destroyed if droplet particles stopped moving or fell into the ground. The volume V_d of all the droplet particles deposited on the grass blade.

4) Rendering. All the droplet particles were rendered according to the updated particle properties and then returned to step 2. The algorithm was terminated after all droplet particles were destroyed.

Furthermore, the Oriented Bounding Box algorithm[18] was used to detect the collision between the droplet and the blade.

2.2 Droplet motion

The following rules were applied in this study: 1) droplets were formed at the nozzle orifices; 2) droplets were considered as spheres[19], and the deformation of droplets was neglected during movement in the air; 3) evaporation of the droplet was not taken into account. The spray nozzle was installed under the drone, and the nozzle would spray droplets when staying in working mode in the air (Figure 3). The initial position P_0 for the droplet provides the coordinates of the spray nozzle, and the initial velocity V_0 (m/s) of the droplet can be calculated using Equation (2).

$$\vec{V}_0 = \vec{V}_s + \vec{V}_m \tag{2}$$

where, V_s is the spray velocity of the droplet relative to the nozzle, and V_m is the moving velocity of the drone, m/s. According to the specified nozzle model, the diameter of droplets D and V_s can be obtained[20].

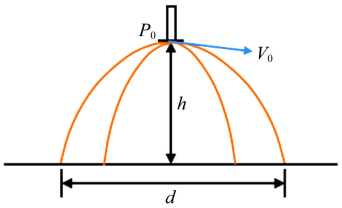

Note: Motion curve of droplets designated by orange lines. h indicates the height of the nozzle from the ground, and d is the diameter of the sprinkled area.

Figure 3 Motion trail of droplets

When the droplets move in the air, they are affected by gravity G, air resistance F_d, and natural wind force F_w (as shown in Figure 4). According to Newton's law of motion, the displacement A of the droplet with time t is expressed as:

$$m\frac{\partial^2 A}{\partial t^2} = \vec{G} + \vec{F}_d + \vec{F}_w \tag{3}$$

$$m = \frac{\pi}{6}\rho_d D^3 \tag{4}$$

where, m, D, and ρ_d are the mass (kg), the diameter (m), and the density of the droplet (kg/m^3), respectively. According to the initial conditions (Equations (5) and (6)), the relationship between the displacement A (m) of the droplet and the time t (s) can be calculated by the following:

$$A\big|_{t=0} = 0 \tag{5}$$

$$\frac{\partial A}{\partial t}\Big|_{t=0} = V_0 \tag{6}$$

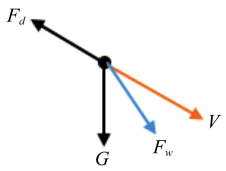

Figure 4 Force analysis of the droplets in the air

2.3 Interaction

During the collision of the droplet with the foliage, the energy changes in a complicated way. The droplets, which possess kinetic energy and surface energy before the collision, are subjected to impact pressure, making them spread on the leaf surface, and eventually becoming disk shaped. During this process, the kinetic energy of the droplet is converted into surface energy. After the diameter of the droplet spread reaches its maximum, according to the surface energy of the droplet at this time, it can be estimated whether the droplet is broken or not. If the droplet does not break, it then begins to shrink under the effect of surface tension, and the surface energy gradually transforms into kinetic energy, which means that the droplet may eventually be deposited on the foliage or else bounce.

Mao et al.[21] proposed an algorithm to calculate the probability of the droplets rebounding considering the energy changes during the processes of droplets and foliar impact. However, their study only considered the situation where the drop hits the plane perpendicularly from above, and calculates the effect when the leaf is tilted. Dorr et al.[22] extended the method showing how it can be determined whether droplets rebound or not, by taking into account the remaining energy E_r. For the fragmentation of droplets, they proposed a fragmentation factor e ($0<e\leq1$) and a fixed parameter p ($0\leq p<1$) to denote the period and degree of fragmentation of the droplet, respectively. When f equals one, the droplet is broken at the maximum expanded diameter, whereas when p equals 0, the droplet is completely crushed. On the other hand, $p>0$ means the droplet is partially broken with some portion of the droplet remaining on the leaf. However, there is no reliable way to determine the optimal values of e and p. In this study, the Weber number (W_e) was used as the conditions for rebound, settlement, and fragmentation of the droplet[23-25]. A rebound occurs when $W_e<30$, and droplets deposit on the target when ($30\leq W_e<80$); lastly, sputtering occurs when $W_e\geq80$. W_e was calculated by the equation as follows:

$$W_e = \frac{\rho V^2 l}{\sigma} \tag{7}$$

where, ρ is the fluid density, kg/m^3; V is the characteristic flow rate, m/s; l is the characteristic length, m; σ is the surface tension coefficient of the fluid, N/m.

According to Mao et al.[21], the velocity after the droplet bounces V_{exit} (m/s) is

$$V_{exit} = \sqrt{\frac{12E_r}{\pi\rho D^3}} \tag{8}$$

where, E_r is the residual energy of the droplet, J.

Because there may be some fine fluff on the surface of the blade, the fluff will produce a drag force on the droplet when the latter bounces. Therefore, the residual energy of the droplet bounce E_r needs to be reduced by the energy E_D required for overcoming the drag force. A coefficient k ($0<k<1$) was defined to calculate the remaining energy of the droplet after removing the energy E_D required by the tractable drag force. With introducing the coefficient k into Equation (8), the modified rebound speed of the droplet V'_{exit} can be expressed as,

$$V'_{exit} = \sqrt{\frac{12kE_r}{\pi\rho D^3}} \tag{9}$$

2.4 Optimization

Based on the previous analysis process, two main factors affecting the spraying efficiency are the flight speed and the altitude of the drone. The experimental results are also different under various parameter settings. The standard Particle Swarm Optimization (PSO) algorithm[16] was used in this study to optimize these two parameters. The Particle Swarm Optimization[26]

algorithm, which is inspired by the regularity of the activities of bird flocking, is a simplified model based on swarm intelligence. The particle swarm algorithm is a global random search algorithm based on swarm intelligence, which is inspired by the results of artificial life research and simulates migration and clustering behavior of foraging birds. Figure 5 shows the basic frame of the algorithm.

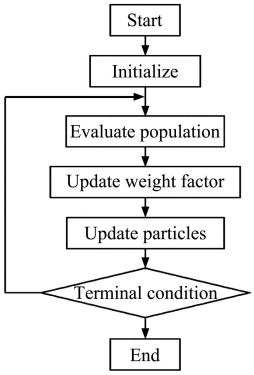

Figure 5 Basic decision tree of the Particle Swarm Optimization algorithm

The droplet deposition rate and the uniformity of droplet deposition distribution are the main criteria for evaluating spray effect. The final droplet deposition rate was chosen to be the fitness value f of the optimization procedure:

$$f = \frac{V_d}{V_a} \times 100\% \tag{10}$$

where, V_d is the volume of all droplets that deposit on the leaf surface after the UAV stops working (m^3), and V_a is the total volume of all droplets (m^3). After each iteration, the individual previous optimal value and population optimal value are updated. The particle update equation[16] is as follows:

$$v_i(T+1) = \omega \cdot v_i(T) + c_1 \cdot r_1 \cdot (p_i(T) - x_i(T)) + c_2 \cdot r_2 \cdot (p(T) - x_i(T)) \tag{11}$$

$$x_i(T+1) = x_i(T) + v_i(T+1) \tag{12}$$

$$\omega = \omega_{\max} - \frac{(\omega_{\max} - \omega_{\min}) \cdot T}{T_{\max}} \tag{13}$$

where, $v_i(T)$ is the velocity of the i-th particle at iteration step T; $x_i(T)$ represents the position of the i-th particle at iteration step T; ω is the inertia weight factor; c_1 is the local weight factor (c_1=2); c_2 is the global weight factor (c_2=2); r_1 and r_2 are random values in the range [0, 1]; $p_i(T)$ is the historically best solution of the i-th particle; $p(T)$ is the historically optimal solution at the population level; $\omega_{\max}$ is the maximum inertia weight; $\omega_{\min}$ is the minimum inertia weight; T is the current number of iterations; $T_{\max}$ is the maximum number of iterations.

Several different flight altitude values were used in the usual range of UAV flight altitudes. PSO was used to obtain the optimal flight speed based on each flight altitude value. Finally, the experimental results were compared to obtain a set of optimal parameters. The optimization workflow consisted of the following steps:

Step 1: The population is initialized to generate at random the position and velocity of all particles in the population within a given range. The drone's flight speed range is set to 4-8 m/s, and the flight altitude is selected from 1 m, 2 m, 3 m, and 4 m above the ground.

Step 2: Drone flight route setting. The target area is a rectangular area without obstacles. Calculate the sprinkling width d as a function of flight altitude and speed, and set the drone flight route according to d and crop size (as shown in Figure 6). The drone takes off from the lower boundary, with the distance between the takeoff point and the left boundary being d/2, flies towards the upper boundary along the dotted line, and then turns right and flight with a distance of d. This route planning method is applicable to the work area without obstacles[27].

Step 3: Start iterating. The position and velocity of the particle are updated according to the updated formulas (Equations (11) and (12)). After each iteration is completed, the fitness value f is calculated. The optimal value of the population and the individual optimal values of the particles are updated.

Step 4: The algorithm stops after the maximum number of iterations (set to 200) is attained.

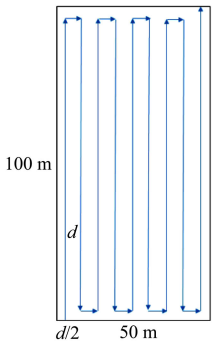

Figure 6 Schematic diagram of the flight path of the drone. The dashed line indicates the flight route of the drone (Ground size is set to 50 m×100 m)

3 Results

3.1 Verification of the particle deposition model

Comparative experiments were conducted to prove the accuracy of the particle deposition model used in the study. Simulation experiments were carried out with our model and comparison model[22]. The simulation results were compared with measured data[22]. Five different nozzles were used in the experiment. The detailed parameters of nozzles are listed in Table 1. The nozzle is 50 cm high from the plant, and the velocity of the nozzle is 1.1 m/s. The fat hen was used as the target crop, and a spray test was carried out with different nozzles. As shown in Figure 7, the results obtained with the model proposed within this study are closer to the measured value compared with the comparison model.

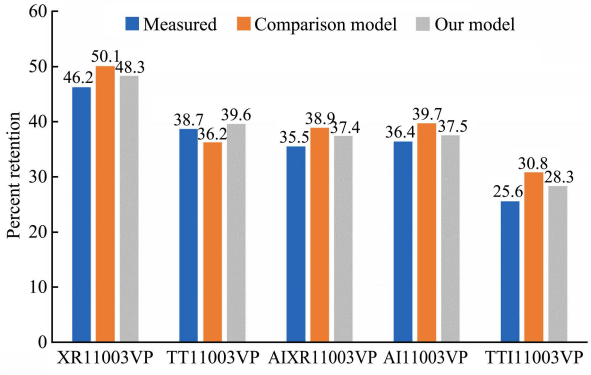

Figure 7 Comparison of the Retention Percentage from measured data, comparison model, and our model with five different nozzles

3.2 Parameters optimization

In this study, the standard PSO algorithm was used to optimize the drone spray parameters for a population size of 50. The inertia-weighting factor adopts the linearly decreasing weighting strategy[16], which ensures that at the beginning of the algorithm,

the particles can explore a wider region in a global range at a higher speed.

Table 1 Detailed parameters of different nozzles

Nozzle	Spray formulation	Droplet spectra/μm	Relative span	Initial velocity/m·s^{-1}
XR11003VP	Water	202	1.28	20.1
TT11003VP	Water	412	1.48	17.1
AIXR11003VP	Water	436	1.12	15.5
AI11003VP	Water	599	1.09	13.3
TTI11003VP	Water	833	1.18	9.1

In the later stage of the search, the smaller weights can ensure that the particles do a fine search around the extreme points so that the algorithm has a larger probability to converge toward the position of the global optimal solution. In all experiments, the model of the nozzle is XR11001VS[28] and the liquid flow rate is 0.379 L/min.

Figure 8 shows that as the number of iterations increases, the fitness of individuals in the population tends to stabilize. After the number of iterations reaches 50, the fitness value of individuals changes only a little. The final deposition rate can reach up to 60%. The deposition rate of the droplets is used as a criterion for evaluating the parameters of the drone operating parameters. It can be observed that as the number of iterations increases, the droplet deposition rate gradually increases, indicating that our algorithm is effective. Figures 8a-8d show the results of four experiments with different values of flight altitude. From the similarity of the results, it can be observed that our algorithm is stable.

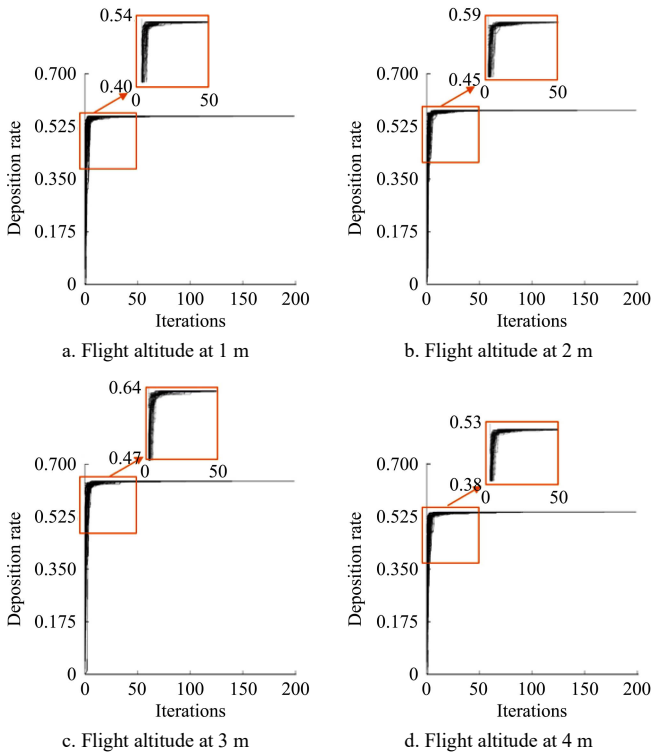

a. Flight altitude at 1 m b. Flight altitude at 2 m

c. Flight altitude at 3 m d. Flight altitude at 4 m

Note: The number of curves in each subfigure is 50. A single curve represents the relationship between the deposition rate of an individual in PSO and the number of iterations.

Figure 8 Relationship between the deposition rate of particles and the number of iterations

Figure 9a shows the relationship between flight height and droplet deposition rate when the flight velocity is set to 4 m/s. It can be observed that the droplet deposition rate changes little when the flying height is in the range of 1-3 m. The droplet deposition rate increases from 16.08% to 20.03%, and the rate of increase is 24.56%. When the flying height range is 3-5 m, the droplet deposition rate increases with the increase in flying height. The droplet deposition rate increases from 16.08% to 52.19%, and the rate of increase is 224.56%. When the flying height is 4.8 m, the droplet deposition rate reaches a maximum of 53.06%.

Figure 9b shows the relationship between flight velocity and droplet deposition rate when the flight altitude is 5 m. It can be observed that the droplet deposition rate shows an upward trend when the flight velocity is in the range of 1-2 m/s. The droplet deposition rate increases from 16.65% to 20.14%, and the rate of increase is 20.96%. When the flying speed is in the range of 2-3 m/s, the droplet deposition rate changes little. When the flying velocity is in the range of 3-6 m/s, the droplet deposition rate increases sharply with the increase in flight velocity. The droplet deposition rate increases from 20.02% to 53.41%, and the rate of increase is 166.78%. The droplet deposition rate reached a maximum of 54.23% at a flight velocity of 5.8 m/s. Figure 9 shows the deposition rate for different values of flight altitude and flight velocity. Since the interaction between droplets and the leaf surface is stochastic, for the same values of flight altitude (5 m) and flight velocity (4 m/s), Figures 9a and 9b show a different deposition rate.

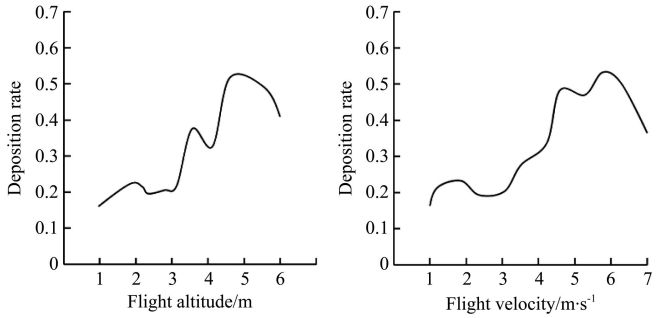

a. Flight altitude b. Flight velocity

Figure 9 Influence of flight altitude and velocity on the droplets deposition rate

As shown in Figure 10, the wind was added to the experiment. The wind velocity was set to 3 m/s in Figure 10a and 6 m/s in Figure 10b. The flight altitude is uniformly designated as 2 m. After the number of iterations reaches 70, the algorithm begins to converge. The convergence rate of the algorithm is slower. Compared with the original results, the droplet deposition rate has also changed.

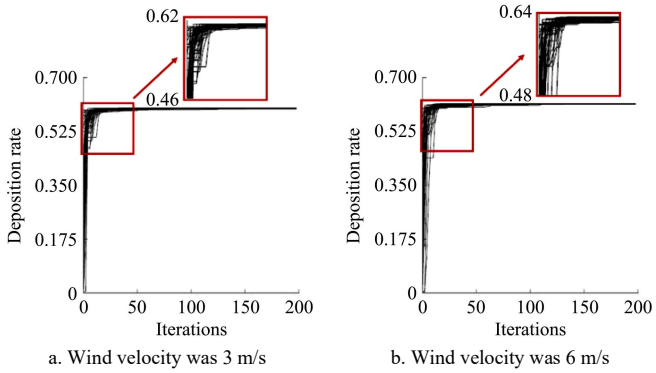

a. Wind velocity was 3 m/s b. Wind velocity was 6 m/s

Figure 10 Schematic diagram of droplets deposition rate affected by wind

4 Discussion

Faical et al.[14] investigated a methodology based on PSO for fine-tuning the control rule of the UAV. The use of this methodology increases the precision of spraying pesticides. However, the deposition characteristics of droplets have not been taken into account. Although the product is within a target crop field, there are still droplets wasted. In this study, a physics-based method was used to simulate the interaction between droplets and plants. Indeed, there will be a gap between the field performance and the simulation results, since there are a few assumptions made within the algorithm implementation, among which the simplified plant organs may take the major role. Take fluff on the leaf blade surface as an example: there is currently no precise method to calculate the energy required for the droplet to overcome the drag generated by the fluff. The value of the coefficient k set in the experiment is not very accurate. In this paper, the Weber number was used to describe the conditions for rebound, settlement, and crushing of droplets. In a number of studies[20,21,27,28], various crushing conditions of the droplets were proposed, and one of the conditions specifically considered needs to be decided based on the actual situation.

In this study, the flight altitude and flight speed of the UAV are selected as the parameters to be optimized. In the experiment, several specific flying altitude values were selected to optimize the flight speed. In actual operations, one flight mode is that the UAV flies at a fixed altitude. The other is that the flight altitude of the UAV can change along with the terrain. The flight altitude refers to the altitude of UAV relative to the horizontal plane. If the terrain is undulated and sloped, accidents may occur when the altitude changes during the flight of the UAV. If the flight altitude and flight speed are optimized at the same time, the terrain needs to be considered at the same time. And in the optimization result, the flight altitude is not a fixed value. The flight altitude can be changed many times during one operation, which increases the potential safety hazards.

The final deposition rate of the droplets was used as a fitness function during the optimization process, while the flight time of the drone was not considered. The purpose of optimizing drone flight parameters is to obtain the lowest spray cost. To achieve this goal, the efficiency of the pesticide needs to be increased, while the operating time of the drone is reduced. In other words, the best spray effect with the least amount of liquid in the shortest time means the lowest spray cost. However, there is no good way to quantify the time factor. In addition, the uniformity of the droplet deposition distribution is also a criterion for evaluating the spray effect. Increasing the uniformity of the droplet distribution means reducing the spray repetition rate.

5 Conclusions

In this study, a 3D-simulation-based optimization method for plant-maintenance UAV flight parameters was proposed. This method can optimize the UAV operating parameters to obtain the best flight parameters with different environmental conditions such as wind velocity, variety of crops, and size of spray area. As there still are some errors in simulating the interaction process between the droplet and the leaf blade, the interaction algorithm between the droplet and the plant can be modified in the future to fit in more reality. It is also conceivable to find a way to quantify the time cost and to add the UAV operating time factor to the design of the fitness function of the optimization algorithm.

Acknowledgements

This work was financially supported by the National Natural Science Foundation of China (Grant No. 32271983; No. 61571400). The financial supports were gratefully acknowledged.

[References]

[1] Archambault S. Ecological modernization of the agriculture industry in southern Sweden: Reducing emissions to the Baltic Sea. J Clean Prod., 2004; 12(5): 491–503.

[2] Yuan L, Zhang H B, Zhang Y T, Xing C, Bao Z Y. Feasibility assessment of multi-spectral satellite sensors in monitoring and discriminating wheat diseases and insects. Optik, 2017; 131: 598–608.

[3] Mottes C, Jannoyer M L, Bail M L, Guéné M, Carles C, Malézieux E. Relationships between past and present pesticide applications and pollution at a watershed outlet: The case of a horticultural catchment in Martinique, French West Indies. Chemosphere, 2017; 184: 762–773.

[4] Tokekar P, Hook J V, Mulla D, Isler V. Sensor planning for a symbiotic UAV and UGV system for precision agriculture. IEEE Trans Robot, 2016; 32(6): 1498–1511.

[5] Xu B, Chen L P, Tan Y, Xu M. Rout planning algorithm and verification based on UAN operation path angle inirregular area. Transactions of the CSAE, 2015; 31(23): 173–178. (in Chinese)

[6] Zhang S C, Qiu B J, Xue X Y, Sun T, Peng B. Parameters optimization of crop protection UAS based on the first industry standard of China. Int J Agric & Biol Eng, 2020; 13(3): 29–35.

[7] Franz E, Bouse L F, Carlton J B, Kirk I W, Latheef M A. Aerial spray deposit relations with plant canopy and weather parameters. Transactions of the ASAE, 1998; 41(4): 959–966.

[8] Lan Y B, Hoffmann W C, Fritz B K, Martin D E, Lopez J D. Spray Drift Mitigation with Spray Mix Adjuvants. Appl Eng Agric, 2008; 24(1): 5–10.

[9] Kirk I W. Measurement and prediction of atomization parameters from fixed-wing aircraft spray nozzles. Transactions of the ASABE, 2007; 50(3): 693–703.

[10] Fritz B K, Hoffmann W C. Update to the USDA-ARS fixed-wing spray nozzle models. Transactions of the ASABE, 2015; 58(2): 281–295.

[11] Fritz B K, Hoffmann W C, Bagley W E, Kruger G R, Czaczyk Z, Henry R S. Influence of air shear and adjuvants on spray atomization. ASTM Int., 2014; 33: 151–173.

[12] Huang Y, Zhan W, Fritz B K, Thomson S J. Optimizing selection of controllable variables to minimize downwind drift from aerially applied sprays. Appl Eng Agric, 2012; 28(3): 307–314.

[13] Faical B S, Pessin G, Filho G P R, Carvalho A C P L F, Furquim G, Ueyama J. Fine-tuning of UAV control rules for spraying pesticides on crop fields. Proc ICTAI, 2014; pp.527–533.

[14] Faical B S, Pessin G, Filho G P R, Furquim G, de Carvalho A C P L F, Gomes P H, et al. Exploiting evolution on UAV control rules for spraying pesticides on crop fields. Communications in Comput Information Science, 2014; 459: 49–58.

[15] Hou C J, Tang Y, Luo S M, Lin J T, He Y, Zhuang J J, et al. Optimization of control parameters of droplet density in citrus trees using UAVs and the Taguchi method. Int J Agric & Biol Eng, 2019; 12(4): 1–9.

[16] Shi Y H, Eberhart R. A modified particle swarm optimizer. Proc ICEC, 1998; pp.69–73.

[17] Mohammad S, Jonatan A, Ian J, Chen N, Vladimir O. On new triangle quadrature rules for the locally corrected Nyström method formulated on NURBS-Generated Bézier Surfaces in 3-D. IEEE Trans Ante Prop, 2016; 64(7): 3027–3038.

[18] Ding S, Mannan M A, Poo A N. Oriented bounding box and octree based global interference detection in 5-axis machining of free-form surfaces. Comput-Aided Design, 2004; 36(13): 1281–1294.

[19] Edling R. Kinetic energy, evaporation and wind drift of droplets from low pressure irrigation nozzle. Transactions of the ASAE, 1985; 28(5): 1543–1550.

[20] Dorr G J, Hewitt A J, Adkins S W, Hanan J, Zhang H C, Noller B. A comparison of initial spray characteristics produced by agricultural nozzles. Crop Prot., 2013; 53: 109–117.

[21] Mao T, Kuhn D C S, Tran H. Spread and rebound of liquid droplets upon impact on flat surfaces. AlChE Journal, 1997; 43(9): 2169–2179.

[22] Dorr G J, Forster W A, Mayo L C, McCue S W, Kempthorne D M, Hanan J, et al. Spray retention on whole plants: modelling, simulations and experiments. Crop Prot, 2016; 88: 118–130.
[23] Wang D M, Watkins A P. Numerical modeling of diesel spray wall impaction phenomena. Int J Heat Fluid Flow, 1993; 14(3): 301–312.
[24] Roisman I V, Tropea C. Fluctuating flow in a liquid layer and secondary spray created by an impacting spray. Int J Multiph Flow, 2005; 31(2): 179–200.
[25] Roisman I V, Horvat K, Tropea C. Spray impact: Rim transverse instability initiating fingering and splash, and description of a secondary spray. Phys Fluids, 2006; 18(10): 102–104.
[26] Kennedy J, Eberhart R. Particle swarm optimization. Proc ICCN95, 1995; pp.1942–1948.
[27] Choset H. Coverage of known spaces: The boustrophedon cellular decomposition. Auton Robot, 2000; 9(3): 247–253.
[28] Xu Y, Bao J, Fu D, Zhu C. Design and experiment of variable spraying system based on multiple combined nozzles. Transactions of the CASE, 2016; 32(17): 47–54. (in Chinese)